

Electronic Supplementary Information (ESI)

A non-luminescent Eu-MOF-based “turn-on” sensor towards anthrax biomark through single-crystal to single-crystal phase transition

Dai Wu,^[a] Zhe Zhang,^[a] Xiwen Chen,^[a] Lingkun Meng,^[a] Chunguang Li,^[a] Guanghua Li,^[a] Xiaobo Chen,^[b] Zhan Shi,^{[a]} and Shouhua Feng^[a]*

^[a] State Key Laboratory of Inorganic Synthesis and Preparative Chemistry, College of Chemistry, Jilin University, Changchun, 130012, P.R. China

^[b] School of Engineering, RMIT University, Carlton, VIC 3053, Australia

1. Experimental section

Materials and Methods

NH₂BTC was synthesized prepared according to the previous reports.¹ All other reagents and solvents were obtained from commercial sources and used without further purification. Elemental analyses were performed on a PerkinElmer 2400 element analyzer. (PXRD) data were obtained using a Rigaku D/Max 2550 automated diffractometer (Cu-K α , 1.5418 Å). IR spectra were measured with KBr pellets on a Bruker IFS-66 V/S FT-IR spectrometer. TG measurement was performed on pre-weighed samples in a nitrogen stream using a Netzsch STA 449C apparatus with a heating rate of 10 °C min⁻¹. The luminescence spectra of the samples were recorded on an Edinburgh Instruments FLS920 spectrofluorimeter equipped with both continuous (450 W) and pulsed xenon lamps. Low-pressure N₂ gas sorption experiments at 77 K were carried out on a Micrometrics ASAP 2020 volumetric gas sorption instrument. Before gas adsorption measurements, the samples were heated to 250 °C for 3 h to completely remove the solvent molecules.

Synthesis of Eu(C₉H₄O₆N)(H₂O)·(H₂O)(DMF)₂ (MOF 1)

Eu(NO₃)₃·6H₂O (44.7 mg, 0.1 mmol) and NH₂BTC (22.5 mg, 0.1 mmol) in a mixed solvent of DMF (3 mL), ethanol (EtOH, 3 mL), and H₂O (2 mL) were placed in a sealed vial (20 mL) and heated to 80 °C for 24 h. The resulting colorless needle crystals were obtained, after being washed by DMF, yield 45.1 mg (81% based on Eu³⁺). Elemental analysis: Anal. Calcd (%) for Eu(C₉H₄NO₆)(H₂O)·(H₂O)(DMF)₂ (*M*_r = 558.33): C, 32.26; H, 4.33; N, 7.52. Found (%): C, 32.28; H, 4.35; N, 7.50. NH₂-MOF-76(Ln) (Ln= Gd, Tb) were synthesized following similar conditions.

Synthesis of Eu(C₉H₄O₆N)(H₂O)·(DMF)_{1.5} (MOF 2)

Normally, crystals of **MOF 1** (100mg) was immersed in EtOH solution of DPA (20mL, 100 μM) at room temperature for 5 days. The resulting colorless needle crystals were collected, after being washed with EtOH and DMF. An approximate yield of 80% was estimated. Elemental analysis: Anal. Calcd (%) for Eu(C₉H₄NO₆)(H₂O)·(DMF)_{1.5} (*M*_r = 501.76): C, 32.38; H, 3.22; N, 6.99. Found (%): C, 32.41; H, 3.24; N, 6.96.

X-ray crystal structure determination:

Data collections were performed at 299 K on a Bruker Apex II CCD diffractometer equipped with graphite-monochromated Mo-K α radiation (λ = 0.71073 Å). Data processing was accomplished with the SAINT program. Structures were solved using direct methods (SHELXT, Olex2) and then refined using SHELXL-2014 and Olex2 to convergence.² Anisotropic displacement parameters were applied to all non-hydrogen atoms. Hydrogen atoms were located geometrically and were added to the structure factor calculation. The formulas for **MOF 1** and **MOF 2** were determined by combining single-crystal structure, elemental microanalysis and TGA. A summary of the crystallographic data for these title complexes is listed in Table S1. Selected bond lengths and angles are shown in Table S2 and Table S3. CCDC-1957993 and CCDC-1957994 contain the supplementary crystallographic data for this paper. This data can be obtained free of charge from The Cambridge Crystallographic Data Centre via www.ccdc.cam.ac.uk/data_request/cif.

Fluorescence measurements

To investigate the potential ability of MOF 1 for fluorescence detection, a fully ground sample of **MOF 1** was dispersed with a final concentration of 0.1 mg/mL in ethanol solution, luminescence measurement was taken 2 h later after analyte was injected.

MOF 1 (0.1 mg/mL, 0.1 mL) was placed into a centrifuge tube with different solvents (2.9 mL), including methanol (MeOH), ethanol (EtOH), N,N'-dimethylformamide (DMF), N,N'-dimethylacetamide (DMA), acetone, dichloromethane (CH₂Cl₂), trichloromethane (CHCl₃), hexane, acetonitrile (CH₃CN), 1,4-dioxane, ethyl acetate (EA), tetrahydrofuran (THF). Subsequently the sample tube was taken out and quickly sealed, then the emission spectra were recorded.

For DPA concentration-dependent luminescence measurements were prepared, as follows. **MOF 1** (0.1 mg/mL, 1.5 mL) was placed into a centrifuge tube with various DPA (0-200 μM, 1.5 mL). Subsequently the sample tube was taken out and quickly sealed, then the emission spectra were recorded after 2 h.

In-situ time-dependent luminescent experiments were prepared, as follows. **MOF 1** samples (0.1 mg/mL, 1.5 mL) were added into a testing quartz cuvette, and the DPA (60 μM, 1.5 mL) was injected quickly. Then the luminescence spectra and intensity of MOF sensor versus time plots were obtained.

The application performance of **MOF 1** was investigated for fluorescent paper, as follows. The filter paper was cut square and impregnated with the ethanol solution of **MOF 1** (0.1 mg/mL, 20 mL). After 10 minutes, the filter strip is taken out and dried in air. The testing strip were added to the test solution for 10s to judge the DPA content rapidly by naked eyes with observable fluorescence change under a UV lamp at 254 nm (DPA concentration: 60μM, interferents: 100 μM).

Structure description:

MOF 1

As shown in Fig. 1a, its asymmetric unit consists of one crystallographically independent Eu³⁺ ion, one deprotonated NH₂BTC³⁻ anion and one coordinated water molecule. Eu1 is seven coordination, with six oxygen atoms from the carboxylate groups of the three NH₂BTC ligands and a terminal water molecule, forming a slightly distorted pentagonal bipyramid (Fig. S1a). The deprotonated NH₂BTC³⁻ is connected to six Eu atoms (Fig. S1b). The Eu-O bond lengths are in the range of 2.253(4)-2.460(6) Å within the normal range for this bond (Table. S2), and the Eu-O bond lengths of Eu1-O7(water) is the longest. The infinite Eu-O-C chains are bridged by the benzene ring of the NH₂BTC ligand to form a 3D rod-packing structure along the [001] direction. The rods pack in a tetragonal fashion, resulting in 6.6 × 6.6 Å² square channels in the c direction, which are filled with DMF and H₂O molecules (Fig. S1d).

The structure description of **MOF 2** was similar to **MOF 1** (Fig. S2). As the distance of Eu-O-C rods from each other is different from **MOF 1**, the 1D narrow rectangular channel of about 6.7 × 6.0 Å² along the c axis was formed.

Table S1. Crystallographic data and structure refinement parameters for **MOF 1** and **MOF 2**

compound	MOF 1	MOF 2
Empirical formula	C ₁₅ H ₂₄ EuN ₃ O ₁₀	C _{13.5} H _{16.5} EuN _{2.5} O _{8.5}
Fw	558.33	501.76
Crystal system	tetragonal	tetragonal
Space group	<i>P</i> 4 ₃	<i>P</i> 4 ₃ 2 ₁ 2
Temperature (K)	299.11	299.02
Radiation	MoK α (λ = 0.71073)	MoK α (λ = 0.71073)
<i>a</i> /Å	10.4323(4)	14.564(3)
<i>b</i> /Å	10.4323(4)	14.564(3)
<i>c</i> /Å	14.3109(8)	14.223(4)
α /°	90	90
β /°	90	90
γ /°	90	90
<i>V</i> / Å ³	1557.5(15)	3017.0(15)
<i>Z</i>	4	8
F(000)	728.0	1464.0
Crystal size (mm ³)	0.28×0.13×0.12	0.27×0.12×0.12
ρ_{calcd} (g cm ⁻³)	1.655	1.713
μ (Mo K α)/ mm ⁻¹	4.045	4.177
Reflections collected / unique	12785/2927 [<i>R</i> _{int} = 0.0472]	25159/2089 [<i>R</i> _{int} = 0.062]
<i>R</i> ₁ / <i>wR</i> ₂ (<i>I</i> > 2 σ (<i>I</i>)) ^{a,b}	0.0397/0.1135	0.0392/0.1137
<i>R</i> ₁ , <i>wR</i> ₂ (all data)	0.0460/0.1232	0.0460/0.1232
GOF on F ²	0.976	1.127

$$^a R_1 = \sum ||F_o| - |F_c|| / \sum |F_o|, \quad ^b wR_2 = [\sum w(|F_o|^2 - |F_c|^2)^2 / \sum w(F_o)^2]^{1/2}$$

Table S2. Selected bond lengths and bond angles for **MOF 1**

Eu1-O1	2.296(4)	Eu1-O2 ¹	2.360(5)
Eu1-O3 ²	2.337(5)	Eu1-O4 ³	2.253(4)
Eu1-O5 ⁴	2.419(4)	Eu1-O6 ⁵	2.359(6)
Eu1-O7	2.460(6)		
O7-Eu1-O1	64.0(2)	O7-Eu1-O2 ¹	75.4(2)
O7-Eu1-O3 ²	74.7(3)	O7-Eu1-O4 ³	138.5(2)
O7-Eu1-O5 ⁴	145.4(2)	O7-Eu1-O6 ⁵	81.3(3)

Symmetry transformations used to generate equivalent atoms:

$$^1-2-Y,-1+X,-1/4+Z; \quad ^2-1-X,-2-Y,-1/2+Z; \quad ^3-1-Y,-1+X,-1/4+Z; \quad ^4+X,-1+Y,+Z; \quad ^5+Y,-2-X,1/4+Z.$$

Table S3. Selected bond lengths and bond angles for **MOF 2**

Eu1-O1	2.299(12)	Eu1-O2 ¹	2.335(10)
Eu1-O3 ³	2.378(14)	Eu1-O4 ²	2.253(4)
Eu1-O5 ⁴	2.321(10)	Eu1-O6 ⁵	2.332(11)
Eu1-O7	2.538(19)		
O7-Eu1-O1 ²	142.1(6)	O7-Eu1-O2 ¹	80.9(7)
O7-Eu1-O3 ³	145.2(6)	O7-Eu1-O4	75.7(8)
O7-Eu1-O5 ⁴	68.7(6)	O7-Eu1-O6 ⁵	66.5(6)

Symmetry transformations used to generate equivalent atoms:

$^{1/2}-Y, -1/2+X, -1/4+Z$; $^21-X, -Y, 1/2+Z$; $^31/2+Y, 1/2-X, 1/4+Z$; $^41-Y, -X, 3/2-Z$; $^51/2-X, -1/2+Y, 7/4-Z$.

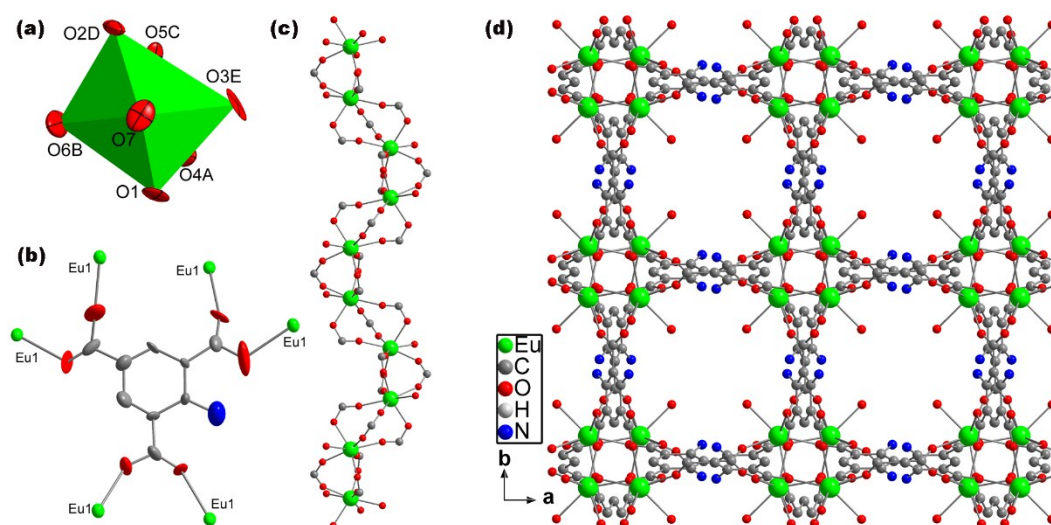


Fig. S1 (a) The polyhedra of Eu of **MOF 1**. Symmetry code for the generated atoms: A $-1-y, -1+x, -0.25+z$; B $y, -2-x, 0.25+z$; C $x, -1+y, z$; D $-2-y, -1+x, -0.25+z$; E $-1-x, -2-y, -0.5+z$. (b) The connected mode of NH_2BTC in **MOF 1**. (c) Ball-and-stick representation of Eu-O-C rod in **MOF 1**. (d) View of the 3D frameworks of **MOF 1** along the $[001]$ direction.

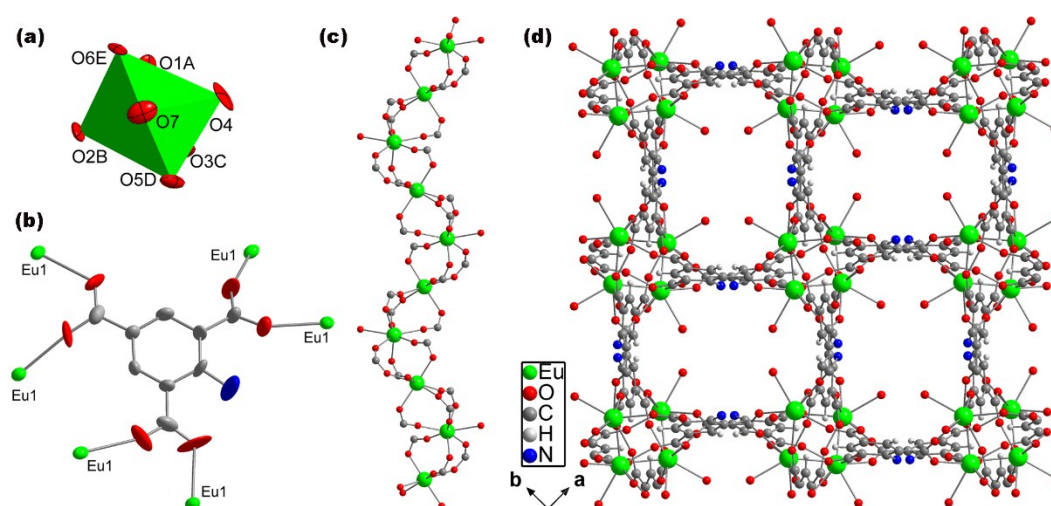


Fig. S2 (a) The polyhedra of Eu of **MOF 2**. Asymmetric codes: A $1/2-Y, -1/2+X, -1/4+Z$; B $1-X, -Y, 1/2+Z$; C $1/2+Y, 1/2-X, 1/4+Z$; D $1-Y, -X, 3/2-Z$; E $1/2-X, -1/2+Y, 7/4-Z$. (b) The connected mode of NH_2BTC in **MOF 2**. (c) Ball-and-stick representation of Eu-O-C rod in **MOF 2**. (d) View of the 3D frameworks of **MOF 2** along the $[001]$ direction.

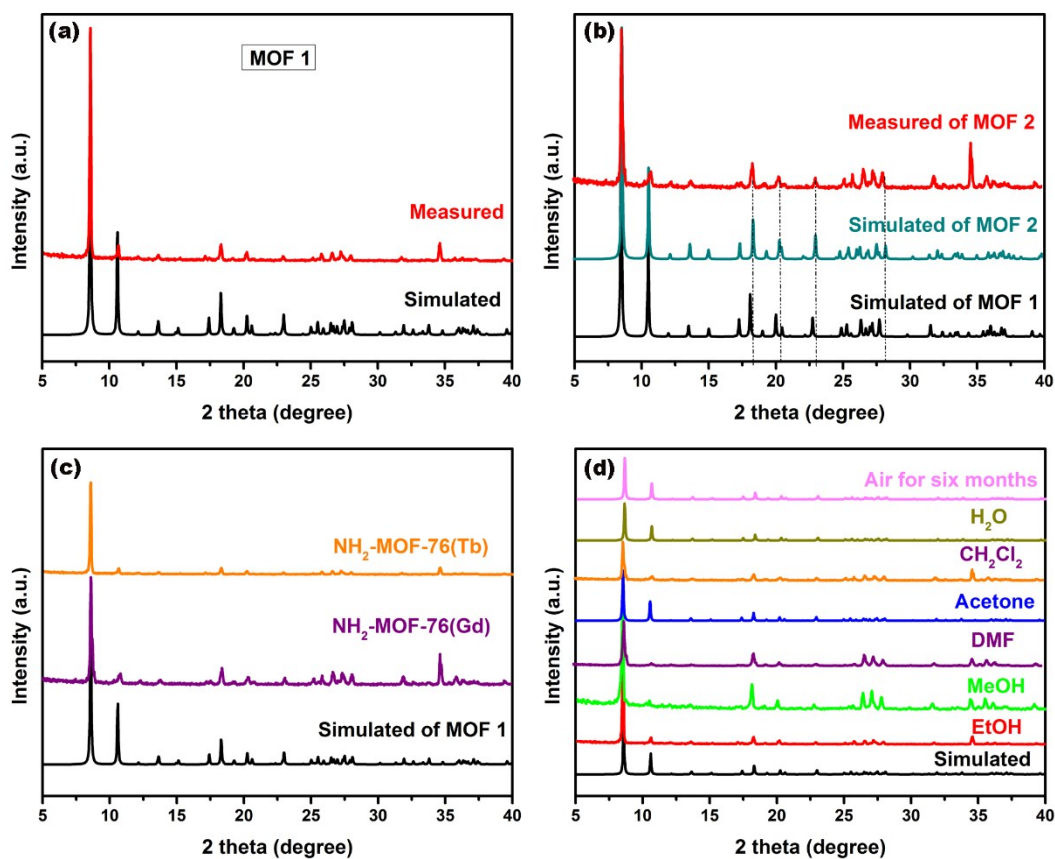


Fig. S3 (a) Simulated and measured XRD powder patterns for compound **MOF 1**. (b) Simulated and measured XRD powder patterns for compound **MOF 2** compared to **MOF 1**. (c) The XRD powder patterns for NH₂-MOF-76(Gd) and NH₂-MOF-76(Tb). (d) The PXRD patterns for **MOF 1** samples after being immersed into various organic solvents and six months in air atmosphere.

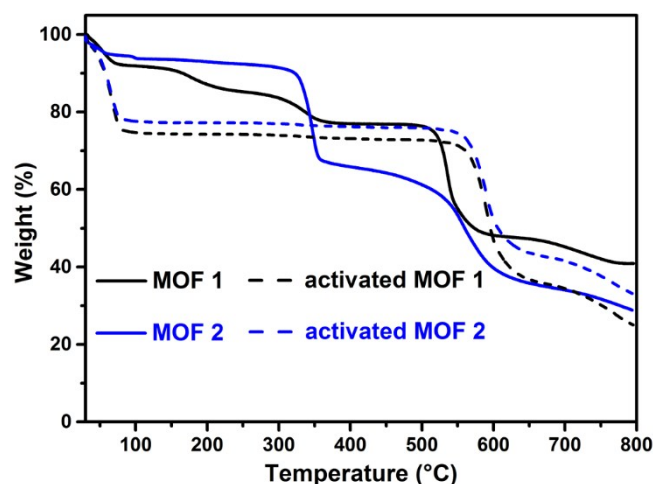


Fig. S4. TGA curves of as-synthesized **MOF-1**, **MOF 2**, activated **MOF 1** and activated **MOF 2** in N₂ flow.

The TGA curves of compound **MOF-1**, **MOF 2**, activated **MOF 1** and activated **MOF 2** under N₂ atmosphere with a heating rate of 10 °C/ min were investigated in the temperature range of 30-800 °C, as shown in Fig. S4.

The TGA curve of **MOF 1** shows four main weight losses. Two water molecules loss is probably

observed till 100°C (found, 7.3%; cald. 6.9%). DMF loss occurs probably in various steps from 100°C to 380°C (found, 26.2%; cald. 25.5%). A rapid loss of nearly 28% is seen in the temperature range 525-625°C, showing loss of organic linker.

For **MOF 2**, one coordinated water molecule loss occurs till 100°C (found, 3.8%; cald. 3.6%). DMF loss occurs probably in various steps from 100°C to 370°C (found, 23.2%; cald. 21.8%). A rapid loss of nearly 25% is seen in the temperature range 420-625°C, showing loss of organic linker.

The TGA curves of the activated **MOF 1** and activated **MOF 2** show the solvent molecules are removed after heating at 250°C in high vacuum.

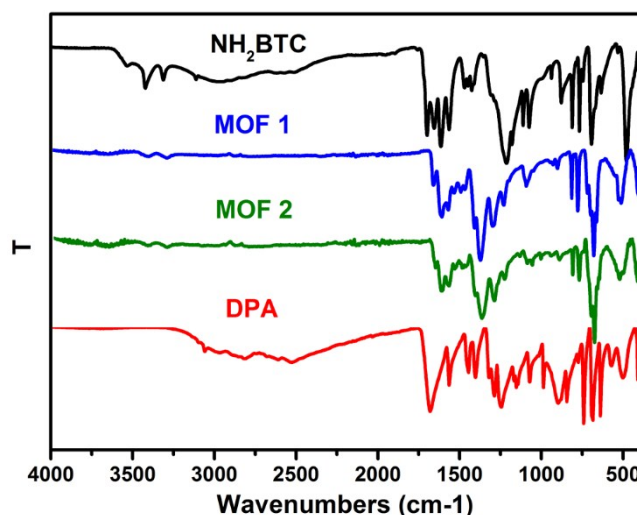


Fig. S5. FT-IR spectra of NH_2BTC , DPA, **MOF 1**, **MOF 2** and activated **MOF 1**.

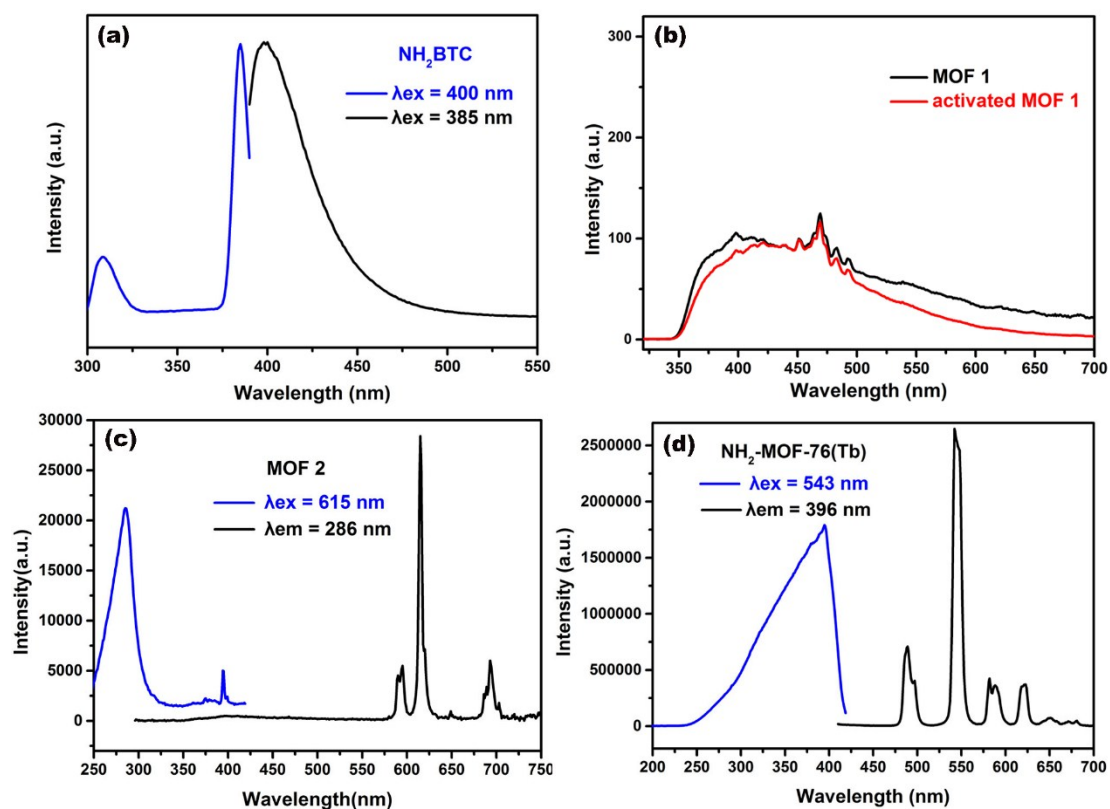


Fig. S6 (a) Solid state excitation and emission spectra of free NH₂BTC ligand. (b), (c) and (d) The solid-state photoluminescence spectrum of **MOF 1**, activated **MOF 1**, **MOF 2** and NH₂-MOF-76(Tb) at room temperature.

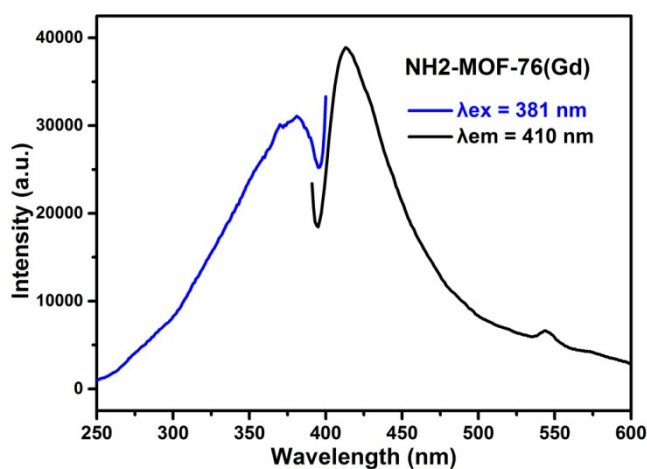


Fig. S7 Solid state excitation and emission spectra of NH₂-MOF-76(Gd) at 77k.

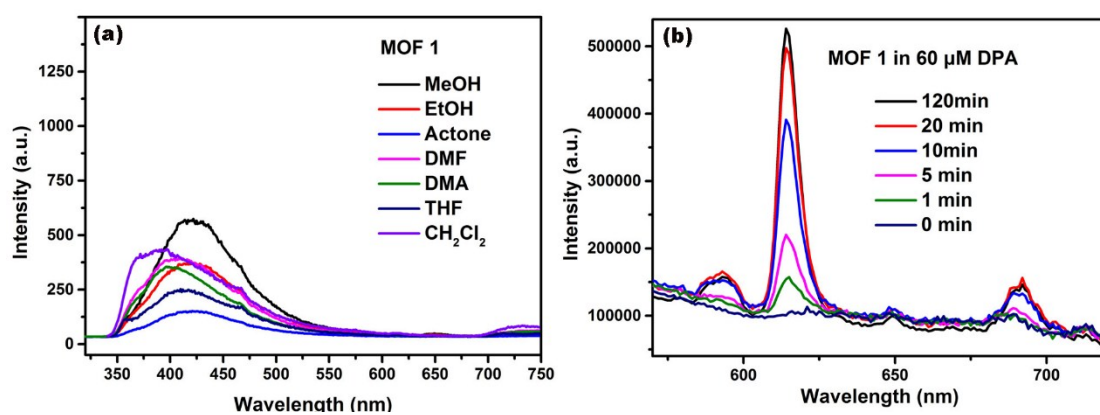


Fig. S8 (a) Emission spectra of **MOF 1** in various solvent solution. (b) Emission spectra of **MOF 1** in EtOH solution under DPA (60 μM) at various time intervals at room temperature (excited at 250 nm).

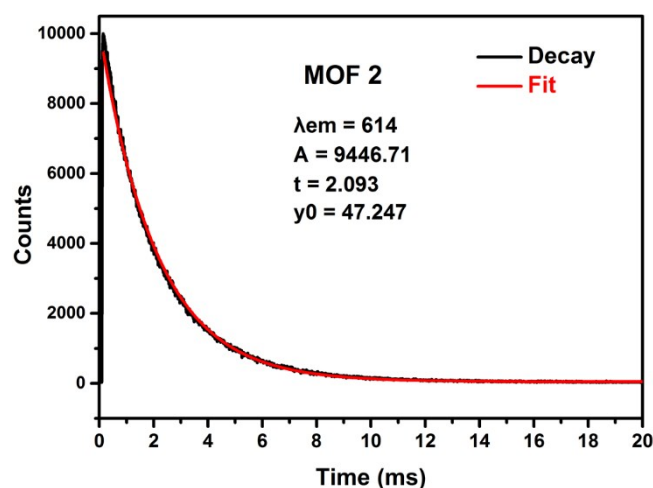


Fig. S9 Luminescence decay curve for the $^5D_0 \rightarrow ^7F_2$ (614 nm) emission of MOF 2.

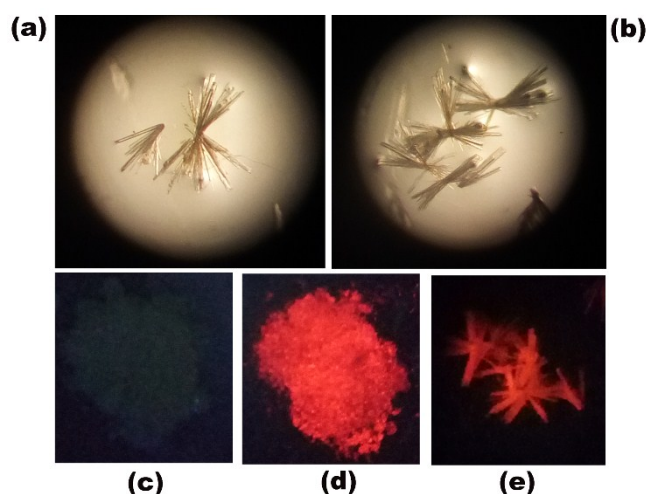


Fig. S10 (a), (b) Crystals photograph of **MOF 1**, **MOF 2** under optical microscopy, respectively. (c), (d) and (e) Luminescence picture of **MOF 1**, **MOF 2** under a UV lamp at 254 nm in dark. (e) Crystals photograph of **MOF 2** under a UV lamp at 254 nm in dark.

Table S4. Performance comparison of several sensors for the detection of anthrax biomark DPA.

Sensor	Detection mechanism	Detection limit	Reference
Eu-MOF (MOF 1)	fluorescence recovery	3.8 μ M	The present work
Tb-COP	turn-on	13.5 nM	<i>Sens. Actuators, B.</i> , 2019, 290 , 9
BODIPY-Cu ²⁺	turn-on	2 μ M	<i>J. Hazard. Mater.</i> , 2019, 377 , 299
PV-Tb ³⁺	dual colorimetric	5 μ M	<i>Analyst.</i> , 2013, 138 , 7079
EBT-Eu ³⁺	dual colorimetric	2 μ M	<i>Anal. Chem.</i> , 2018, 90 , 4221
Tb-based Micelle	turn-on	54 nM	<i>Anal. Chem.</i> , 2018, 90 , 3600
R6H@Eu(BTC)	dual colorimetric	4.5 μ M	<i>Sens. Actuators, B.</i> , 2018, 266 , 263
CDs-Cu ²⁺	on-off-on	12 nM	<i>J. Mater. Chem. C.</i> , 2017, 5 , 6962
Ln(BDC) _{1.5} @SiO ₂	turn-off	48 nM	<i>J. Am. Chem. Soc.</i> , 2007, 129 , 9852

Reference

1. (a) H. N. Rubin and M. M. Reynolds, *Inorg. Chem.*, 2017, **56**, 5266–5274; (b) Y. K. Cai, A. Kulkarni, Y. G. Huang, D. Sholl and K. Walton, *Cryst. Growth. Des.*, 2014, **14**, 6122–6128.
2. (a) G. M. Sheldrick, *Acta Cryst.*, 2015, **A71**, 3-8; (b) O. V. Dolomnov, L. J. Bourhis, R. J. Gildea, J. A. K. Howard and H. Puschmann, *J. Appl Cryst.*, 2009, **42**, 229–341.